BELLE-CONF-0558
EPS05-533

Moments of the Electron Energy Spectrum in $B \to X_c \ell \nu$ decays at Belle

K. Abe,[9] K. Abe,[47] I. Adachi,[9] H. Aihara,[49] K. Aoki,[23] K. Arinstein,[2] Y. Asano,[54] T. Aso,[53] V. Aulchenko,[2] T. Aushev,[13] T. Aziz,[45] S. Bahinipati,[5] A. M. Bakich,[44] V. Balagura,[13] Y. Ban,[36] S. Banerjee,[45] E. Barberio,[22] M. Barbero,[8] A. Bay,[19] I. Bedny,[2] U. Bitenc,[14] I. Bizjak,[14] S. Blyth,[25] A. Bondar,[2] A. Bozek,[29] M. Bračko,[9,21,14] J. Brodzicka,[29] T. E. Browder,[8] M.-C. Chang,[48] P. Chang,[28] Y. Chao,[28] A. Chen,[25] K.-F. Chen,[28] W. T. Chen,[25] B. G. Cheon,[4] C.-C. Chiang,[28] R. Chistov,[13] S.-K. Choi,[7] Y. Choi,[43] Y. K. Choi,[43] A. Chuvikov,[37] S. Cole,[44] J. Dalseno,[22] M. Danilov,[13] M. Dash,[56] L. Y. Dong,[11] R. Dowd,[22] J. Dragic,[9] A. Drutskoy,[5] S. Eidelman,[2] Y. Enari,[23] D. Epifanov,[2] F. Fang,[8] S. Fratina,[14] H. Fujii,[9] N. Gabyshev,[2] A. Garmash,[37] T. Gershon,[9] A. Go,[25] G. Gokhroo,[45] P. Goldenzweig,[5] B. Golob,[20,14] A. Gorišek,[14] M. Grosse Perdekamp,[38] H. Guler,[8] R. Guo,[26] J. Haba,[9] K. Hara,[9] T. Hara,[34] Y. Hasegawa,[42] N. C. Hastings,[49] K. Hasuko,[38] K. Hayasaka,[23] H. Hayashii,[24] M. Hazumi,[9] T. Higuchi,[9] L. Hinz,[19] T. Hojo,[34] T. Hokuue,[23] Y. Hoshi,[47] K. Hoshina,[52] S. Hou,[25] W.-S. Hou,[28] Y. B. Hsiung,[28] Y. Igarashi,[9] T. Iijima,[23] K. Ikado,[23] A. Imoto,[24] K. Inami,[23] A. Ishikawa,[9] H. Ishino,[50] K. Itoh,[49] R. Itoh,[9] M. Iwasaki,[49] Y. Iwasaki,[9] C. Jacoby,[19] C.-M. Jen,[28] R. Kagan,[13] H. Kakuno,[49] J. H. Kang,[57] J. S. Kang,[16] P. Kapusta,[29] S. U. Kataoka,[24] N. Katayama,[9] H. Kawai,[3] N. Kawamura,[1] T. Kawasaki,[31] S. Kazi,[5] N. Kent,[8] H. R. Khan,[50] A. Kibayashi,[50] H. Kichimi,[9] H. J. Kim,[18] H. O. Kim,[43] J. H. Kim,[43] S. K. Kim,[41] S. M. Kim,[43] T. H. Kim,[57] K. Kinoshita,[5] N. Kishimoto,[23] S. Korpar,[21,14] Y. Kozakai,[23] P. Križan,[20,14] P. Krokovny,[9] T. Kubota,[23] R. Kulasiri,[5] C. C. Kuo,[25] H. Kurashiro,[50] E. Kurihara,[3] A. Kusaka,[49] A. Kuzmin,[2] Y.-J. Kwon,[57] J. S. Lange,[6] G. Leder,[12] S. E. Lee,[41] Y.-J. Lee,[28] T. Lesiak,[29] J. Li,[40] A. Limosani,[9] S.-W. Lin,[28] D. Liventsev,[13] J. MacNaughton,[12] G. Majumder,[45] F. Mandl,[12] D. Marlow,[37] H. Matsumoto,[31] T. Matsumoto,[51] A. Matyja,[29] Y. Mikami,[48] W. Mitaroff,[12] K. Miyabayashi,[24] H. Miyake,[34] H. Miyata,[31] Y. Miyazaki,[23] R. Mizuk,[13] D. Mohapatra,[56] G. R. Moloney,[22] T. Mori,[50] A. Murakami,[39] T. Nagamine,[48] Y. Nagasaka,[10] T. Nakagawa,[51] I. Nakamura,[9] E. Nakano,[33] M. Nakao,[9] H. Nakazawa,[9] Z. Natkaniec,[29] K. Neichi,[47] S. Nishida,[9] O. Nitoh,[52] S. Noguchi,[24] T. Nozaki,[9] A. Ogawa,[38] S. Ogawa,[46] T. Ohshima,[23] T. Okabe,[23] S. Okuno,[15] S. L. Olsen,[8] Y. Onuki,[31] W. Ostrowicz,[29] H. Ozaki,[9] P. Pakhlov,[13] H. Palka,[29] C. W. Park,[43] H. Park,[18] K. S. Park,[43] N. Parslow,[44] L. S. Peak,[44] M. Pernicka,[12] R. Pestotnik,[14] M. Peters,[8] L. E. Piilonen,[56] A. Poluektov,[2] F. J. Ronga,[9] N. Root,[2] M. Rozanska,[29] H. Sahoo,[8] M. Saigo,[48] S. Saitoh,[9] Y. Sakai,[9] H. Sakamoto,[17] H. Sakaue,[33] T. R. Sarangi,[9] M. Satapathy,[55] N. Sato,[23] N. Satoyama,[42] T. Schietinger,[19] O. Schneider,[19] P. Schönmeier,[48] J. Schümann,[28] C. Schwanda,[12] A. J. Schwartz,[5] T. Seki,[51] K. Senyo,[23] R. Seuster,[8] M. E. Sevior,[22] T. Shibata,[31] H. Shibuya,[46] J.-G. Shiu,[28] B. Shwartz,[2] V. Sidorov,[2] J. B. Singh,[35] A. Somov,[5] N. Soni,[35] R. Stamen,[9] S. Stanič,[32] M. Starič,[14] A. Sugiyama,[39] K. Sumisawa,[9] T. Sumiyoshi,[51] S. Suzuki,[39] S. Y. Suzuki,[9] O. Tajima,[9] N. Takada,[42] F. Takasaki,[9] K. Tamai,[9] N. Tamura,[31] K. Tanabe,[49] M. Tanaka,[9] G. N. Taylor,[22] Y. Teramoto,[33] X. C. Tian,[36] K. Trabelsi,[8]

Y. F. Tse,[22] T. Tsuboyama,[9] T. Tsukamoto,[9] K. Uchida,[8] Y. Uchida,[9] S. Uehara,[9]
T. Uglov,[13] K. Ueno,[28] Y. Unno,[9] S. Uno,[9] P. Urquijo,[22] Y. Ushiroda,[9] G. Varner,[8]
K. E. Varvell,[44] S. Villa,[19] C. C. Wang,[28] C. H. Wang,[27] M.-Z. Wang,[28] M. Watanabe,[31]
Y. Watanabe,[50] L. Widhalm,[12] C.-H. Wu,[28] Q. L. Xie,[11] B. D. Yabsley,[56] A. Yamaguchi,[48]
H. Yamamoto,[48] S. Yamamoto,[51] Y. Yamashita,[30] M. Yamauchi,[9] Heyoung Yang,[41]
J. Ying,[36] S. Yoshino,[23] Y. Yuan,[11] Y. Yusa,[48] H. Yuta,[1] S. L. Zang,[11] C. C. Zhang,[11]
J. Zhang,[9] L. M. Zhang,[40] Z. P. Zhang,[40] V. Zhilich,[2] T. Ziegler,[37] and D. Zürcher[19]

(The Belle Collaboration)

[1]*Aomori University, Aomori*
[2]*Budker Institute of Nuclear Physics, Novosibirsk*
[3]*Chiba University, Chiba*
[4]*Chonnam National University, Kwangju*
[5]*University of Cincinnati, Cincinnati, Ohio 45221*
[6]*University of Frankfurt, Frankfurt*
[7]*Gyeongsang National University, Chinju*
[8]*University of Hawaii, Honolulu, Hawaii 96822*
[9]*High Energy Accelerator Research Organization (KEK), Tsukuba*
[10]*Hiroshima Institute of Technology, Hiroshima*
[11]*Institute of High Energy Physics, Chinese Academy of Sciences, Beijing*
[12]*Institute of High Energy Physics, Vienna*
[13]*Institute for Theoretical and Experimental Physics, Moscow*
[14]*J. Stefan Institute, Ljubljana*
[15]*Kanagawa University, Yokohama*
[16]*Korea University, Seoul*
[17]*Kyoto University, Kyoto*
[18]*Kyungpook National University, Taegu*
[19]*Swiss Federal Institute of Technology of Lausanne, EPFL, Lausanne*
[20]*University of Ljubljana, Ljubljana*
[21]*University of Maribor, Maribor*
[22]*University of Melbourne, Victoria*
[23]*Nagoya University, Nagoya*
[24]*Nara Women's University, Nara*
[25]*National Central University, Chung-li*
[26]*National Kaohsiung Normal University, Kaohsiung*
[27]*National United University, Miao Li*
[28]*Department of Physics, National Taiwan University, Taipei*
[29]*H. Niewodniczanski Institute of Nuclear Physics, Krakow*
[30]*Nippon Dental University, Niigata*
[31]*Niigata University, Niigata*
[32]*Nova Gorica Polytechnic, Nova Gorica*
[33]*Osaka City University, Osaka*
[34]*Osaka University, Osaka*
[35]*Panjab University, Chandigarh*
[36]*Peking University, Beijing*
[37]*Princeton University, Princeton, New Jersey 08544*

[38]*RIKEN BNL Research Center, Upton, New York 11973*
[39]*Saga University, Saga*
[40]*University of Science and Technology of China, Hefei*
[41]*Seoul National University, Seoul*
[42]*Shinshu University, Nagano*
[43]*Sungkyunkwan University, Suwon*
[44]*University of Sydney, Sydney NSW*
[45]*Tata Institute of Fundamental Research, Bombay*
[46]*Toho University, Funabashi*
[47]*Tohoku Gakuin University, Tagajo*
[48]*Tohoku University, Sendai*
[49]*Department of Physics, University of Tokyo, Tokyo*
[50]*Tokyo Institute of Technology, Tokyo*
[51]*Tokyo Metropolitan University, Tokyo*
[52]*Tokyo University of Agriculture and Technology, Tokyo*
[53]*Toyama National College of Maritime Technology, Toyama*
[54]*University of Tsukuba, Tsukuba*
[55]*Utkal University, Bhubaneswer*
[56]*Virginia Polytechnic Institute and State University, Blacksburg, Virginia 24061*
[57]*Yonsei University, Seoul*

Abstract

We report a measurement of the inclusive electron energy spectrum for charmed semileptonic decays of B mesons in a $140\,\mathrm{fb}^{-1}$ data sample collected on the $\Upsilon(4S)$ resonance, with the Belle detector at the KEKB asymmetric energy e^+e^- collider. We determine the first, second and third moments of the electron energy spectrum for threshold values of the electron energy between 0.4 and 1.5 GeV.

PACS numbers: 12.15.Hh, 11.30.er, 13.25.Hw

INTRODUCTION

The Cabibbo-Kobayashi-Maskawa matrix element $|V_{cb}|$ can be extracted from the inclusive branching fraction for charmed semileptonic B-meson decays $\mathcal{B}(B \to X_c \ell \nu)$[1, 2]. Several studies have shown that the spectator model decay rate is the leading term in a well-defined expansion controlled by the parameter $\Lambda_{\rm QCD}/m_b$. Non-perturbative corrections to this leading approximation arise only at order $1/m_b^2$ and above. The key issue in this approach is the ability to separate non-perturbative corrections, that can be expressed as a series in powers of $1/m_b$, and perturbative corrections, expressed in powers of α_s.

The coefficients of the $1/m_b$ power terms are expectation values of operators that include non-perturbative physics. Different expansions exist, reflecting a difference in the approach used to handle the energy scale μ which separates long-distance from short-distance physics [3].

The shape of the lepton spectrum provides constraints on the heavy quark expansion based on local Operator Product Expansion (OPE) [4], which calculates properties of the $B \to X_c \ell \nu$ transitions. So far, measurements of the electron energy distribution have been made by DELPHI, CLEO, BABAR and Belle collaborations [5, 6, 7, 8]. In this note we report a measurement of the first, second and third moment of the electron energy spectrum with a minimum electron momentum cut ranging between 0.4 and 1.5 GeV/c in the B meson rest frame.

The data used in this analysis were collected with the Belle detector at the KEKB [9] asymmetric energy e^+e^- collider. The Belle [10] detector is a large-solid-angle magnetic spectrometer that consists of a three-layer silicon vertex detector (SVD), a 50-layer central drift chamber (CDC), an array of aerogel threshold Čerenkov counters (ACC), a barrel-like arrangement of time-of-flight scintillation counters (TOF), and an electromagnetic calorimeter comprised of CsI(Tl) crystals (ECL) located inside a super-conducting solenoid coil that provides a 1.5 T magnetic field. An iron flux-return located outside of the coil is instrumented to detect K_L^0 mesons and to identify muons (KLM).

The present results are based on a 140 fb^{-1} data sample collected at the $\Upsilon(4S)$ resonance (on-resonance), which contains 1.5×10^8 $B\bar{B}$ pairs. An additional 15 fb^{-1} data sample taken at 60MeV below the $\Upsilon(4S)$ resonance (off-resonance) is used to perform background subtraction from the $e^+e^- \to q\bar{q}$ process. Events are selected by fully reconstructing one of the B mesons, produced in pairs from $\Upsilon(4S)$ decays.

We used a fully simulated generic Monte Carlo sample equivalent to 2.4 times the on-resonance integrated luminosity. Simulated Monte Carlo events are generated with the EVTGEN event generator, and full detector simulation based on GEANT is applied [11].

EVENT SELECTION

After selecting hadronic events [12], we fully reconstruct the decay of a B meson on one side (tag-side), in the decay modes $B \to D^{(*)}\pi^+, D^{(*)}\rho^+, D^{(*)}a_1^+$, yielding a high purity B meson sample. The following sub-decay modes are reconstructed:

- $\bar{D}^{*0} \to \bar{D}^0\pi^0, \bar{D}^0\gamma$,
- $D^{*-} \to \bar{D}^0\pi^+, D^-\pi^0$,
- $\bar{D}^0 \to K\pi, K\pi\pi^0, K\pi\pi\pi, K_S\pi\pi, K_S\pi^0$ and

- $D^- \to K\pi\pi, K_S\pi$.

For each selected event, we calculate the beam-constrained mass $M_{\rm bc}$ and energy difference ΔE:

$$M_{\rm bc} = \sqrt{(E^*_{\rm beam})^2 - (p^*_B)^2}, \quad \Delta E = E^*_B - E^*_{\rm beam}, \tag{1}$$

where $E^*_{\rm beam}$, p^*_B and E^*_B are the beam energy, the B momentum and the B energy in the centre of mass frame, respectively. Events with $M_{\rm bc} > 5.27$ GeV/c^2 and -0.06 GeV $< \Delta E <$ 0.08 GeV are considered to be signal candidates. The number of events, after continuum subtraction, in the signal region are 63155 ± 931 and 40032 ± 475, B^+ and B^0 candidates, respectively [13].

ELECTRON SELECTION

We search for electrons produced in semileptonic B decays on the "non-tag" side. Particle tracks are selected if they originate from near the interaction vertex. In addition, we measure tracks which pass through the barrel region of the detector, corresponding to an angular acceptance of $35° \leq \theta_{\rm lab} \leq 125°$, where $\theta_{\rm lab}$ is the polar angle of the track relative to the z axis (opposite to the positron beam line).

Tracks that pass the above selection criteria and are not used in the reconstruction of the tag-side B meson are considered as electron candidates. Electron identification is based on a combination of ionisation dE/dx measurements in the CDC, the response of the ACC, the shower shape in the ECL, and the ratio of energy deposited in the ECL to the momentum measured by the tracking system (E/p) [10]. The electron momentum spectrum is corrected by a momentum dependent electron detection efficiency, which includes the detector acceptance as well as the selection efficiency. The momentum of the selected electrons is calculated in the B meson rest frame (p_e^{*B}), exploiting the knowledge of the momentum of the fully reconstructed B. We require $p_e^{*B} \geq 0.4$ GeV/c. The electron yield after these cuts is given in Table I, with a signal purity of 69.6% (50.0%) for B^+ (B^0) tags.

Electrons suffer a loss of energy due to bremsstrahlung radiation in the detector material in front of the calorimeter. This biases the electron energy distribution. Hence, we partially correct for this energy loss by recovering some of the emitted photons to restore the original electron energy. The photon candidate is combined with the electron if the photon energy is below 1 GeV and the angle between the photon and the electron is less than 0.05 radians.

In B^+ decays, prompt semileptonic decays ($b \to x\ell\nu$) of the non-tag side B mesons are separated from cascade charm decays ($b \to c \to y\ell\nu$), based on the correlation between the flavor of the tagging B and the electron charge. In B^0 decays, part of the sample mixes, which flips the correlation to the B^0. Thus in the B^0 sample we do not cut on the electron charge $-$ B flavor correlation.

BACKGROUND SUBTRACTION

The reconstructed electron energy spectrum is contaminated by background processes, which should be evaluated and subtracted from the distribution before the extraction of the moments. The residual background is from:

- continuum background,

- combinatorial background,
- background from secondary decays,
- $J/\psi, \psi(2S)$, Dalitz decays and photon conversions,
- fake electrons.

The shape of the continuum background is derived from off-resonance data, and is normalised using the off- to on-resonance luminosity ratio and cross section difference. To account for low statistics in the off-resonance data we fit an exponential to the distribution, before rescaling. The shape of the combinatorial background is derived from generic $B\bar{B}$ Monte Carlo events where either reconstruction or flavor assignment of the tagged B meson is not carried out correctly. The yield of this background is normalised to the on resonance data $M_{\rm bc}$ side band ($M_{\rm bc} < 5.25$ GeV/c^2), after the continuum background subtraction. We also correct for cases where the fully reconstructed B is correctly tagged, but the electron candidate either is not from a B decay (secondary) or is a mis-identified hadron. These background sources are irreducible; to estimate their magnitude we normalise the $B\bar{B}$ Monte Carlo using a fit to the electron momentum distribution after continuum and combinatorial background subtraction.

The background distribution from $B \to D^{(*)} \to e$ decays are scaled using the latest published branching fractions [17]. Contributions from $J/\psi, \psi(2S)$ decays, photon conversions, and Dalitz decays are small after the track and electron selection cuts. The surviving backgrounds are estimated using Monte Carlo simulation and subtracted along with the major secondary backgrounds. The normalisation for the Monte Carlo yield of secondary and fake leptons is obtained from data by fitting to the lepton momentum distribution in the range 0.3 GeV/$c < p_e^{*B} <$ 2.4 GeV/c. Figure 1 shows the raw electron momentum spectrum with all background contributions overlaid. Table I summarises the number of detected electrons and the contributions from these backgrounds.

TABLE I: Electron yields for $p_e^{*B} \geq 0.4$ GeV/c. The errors are statistical only.

B candidate	B^+	B^0
On Resonance Data	6573 ± 81	5564 ± 75
Scaled Off Resonance	258 ± 48	218 ± 45
Combinatorial Background	1394 ± 38	765 ± 28
Secondary	680 ± 26	1915 ± 44
Background Subtracted	4241 ± 105	2666 ± 102

THE ELECTRON ENERGY SPECTRUM AND THE MOMENTS

The electron energy spectrum is generated via Monte Carlo simulation of $B \to X_c e\nu$ decays with the EVTGEN event generator [11]. The spectrum from $B \to X_c e\nu$ is modelled using four components: $X_c = D$ (ISGW2 [14]), D^* (HQET [15]), higher resonance charm meson states D^{**}(ISGW2) and non-resonant $D^{(*)}\pi$ (Goity and Roberts [16]). To account for the most recent theoretical and experimental results, we reweight the D and D^* components

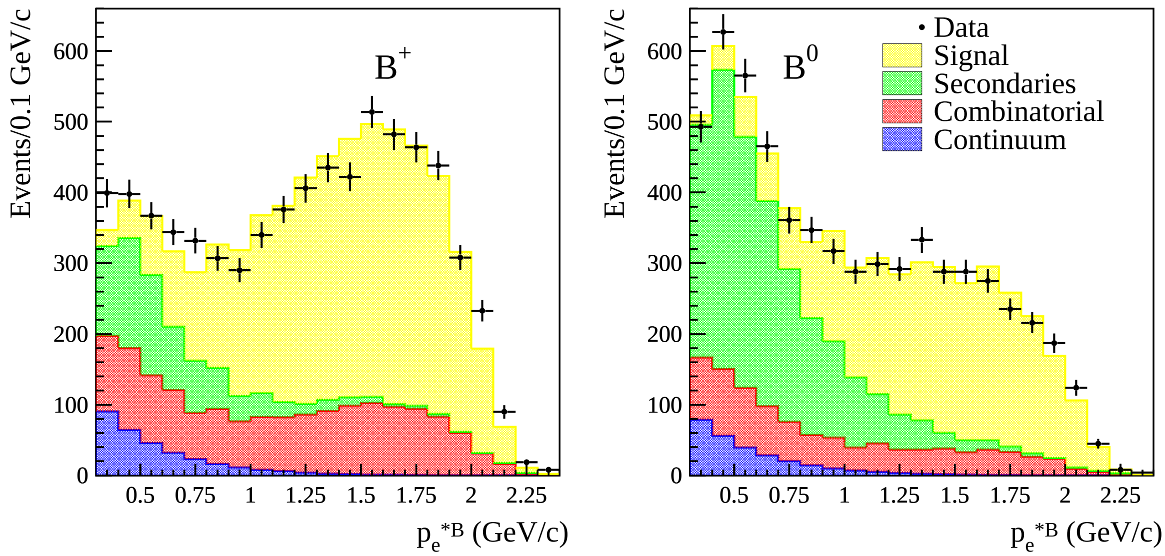

FIG. 1: Breakdown of the backgrounds in the electron momentum spectra for B^+ , and B^0 electrons. The Monte Carlo sample does not include $b \to u$ transitions. The errors shown are statistical only.

in p_e^{*B} to the spectra generated with current (world) average form factors [17]. In addition, the branching fractions for the D and D^* components are corrected according to current (world) average values [17]. Electrons that come from the $b \to u$ transition are subtracted from the unfolded electron energy spectrum, defined later. We model the electron energy spectrum from $B \to X_u l\nu$ transitions using the De Fazio and Neubert prescription [18]. The b-quark motion parameters are derived in Ref. [19]. We scale according to the $B \to X_u l\nu$ branching fraction in Ref. [17].

To measure the first, second and third electron moments we need to determine the true electron energy spectrum in the B meson rest frame, E_e^{*B}. The background subtracted momentum spectrum is distorted by various detector effects. The true electron energy spectrum is extracted by performing an unfolding procedure based on the Singular Value Decomposition (SVD) algorithm [20]. The unfolded spectrum is corrected for QED radiative effects using the PHOTOS algorithm [21], as the OPE does not have an $\mathcal{O}(\alpha)$ QED correction. The unfolded electron energy spectrum is shown in Figure 2.

We measure the central moments of the electron energy spectrum. The first moment is defined to be $M_1^I = \langle E_I \rangle$ and subsequent central moments are determined about the first moment, $M_n^I = \langle (E_I - \langle E_I \rangle)^n \rangle$, where I is the electron energy cutoff and $n = 2, 3$. We measure the first three moments with six electron energy threshold cuts ($I = E_{\rm cut} = 0.4$, 0.6, 0.8, 1.0, 1.2 and 1.5 GeV) combining the spectra from B^+ and B^0 semileptonic decays. Table II provides the final measurements of the moments. Figure 3 shows the moments of the B^0 and B^+ subsamples as a function of $E_{\rm cut}$, as well as the B^0 and B^+ combined average.

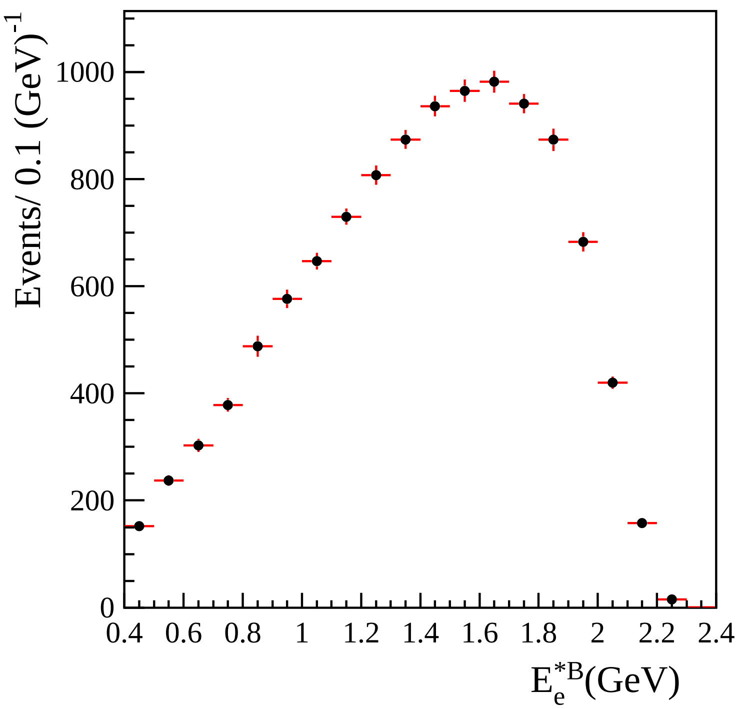

FIG. 2: Unfolded electron energy distribution in the B meson rest frame, combining contributions from B^0 and B^+ decays, and corrected for QED radiative effects. The errors shown are statistical.

SYSTEMATIC UNCERTAINTIES

The systematic uncertainties in the moments stem from event selection, electron identification, background estimation and model dependence.

We determine the electron identification uncertainty from varying the electron identification constraints. In addition, we calculate a systematic uncertainty associated with the electron tracking and detection efficiencies.

Model dependence is estimated from the observed change in the moments when the $B \to De\nu$ and $B \to D^*e\nu$ decay shape parameters are varied according to their uncertainties. The uncertainty in secondary ($B \to D \to e$) decays is derived from switching the branching fraction corrections on and off. Similarly, the correction to the prompt $B \to D^{(*)}e\nu$ branching fraction in the Monte Carlo, incurs such a systematic uncertainty.

The uncertainty due to mis-tagging in the B^0 and B^+ samples is derived from the magnitude of the combinatorial background. Uncertainty in the measured luminosity adds to the uncertainty on continuum electron yield. Additionally we account for the uncertainty associated to magnitude of the hadron fake contribution. The systematic due to the overall fit for the secondaries to the data is estimated by varying the lower p_e^{*B} bound of the fit.

To estimate unfolding uncertainty we vary the effective rank parameter in the SVD algorithm. The uncertainty due to the $b \to u$ subtraction, which occurs after unfolding, is evaluated by varying the normalisation of the De Fazio$-$Neubert inclusive spectrum.

The total systematic error is obtained by adding each contribution in quadrature. It is important to note that the systematic errors are limited by Monte Carlo statistics. The contributions to the systematic error are summarised in Tables III, IV, V for the first, second

and third moments respectively.

TABLE II: Measured moments, M_1, M_2, M_3 and the branching fraction for $B \to X_c e\nu$ in the B meson rest frame for six cutoff energies E_{cut}. The first error is the statistical, and the second error is the systematic. The moments are corrected for QED radiative effects.

E_{cut}[GeV]	M_1[MeV]	M_2[10^{-3}GeV^2]	M_3[10^{-6}GeV^3]
0.4	1397.7 ± 5.1 ± 5.4	172.8 ± 2.4 ± 2.2	-22.4 ± 2.3 ± 0.7
0.6	1431.8 ± 4.8 ± 4.3	148.2 ± 1.9 ± 1.2	-11.6 ± 1.7 ± 0.6
0.8	1481.0 ± 4.4 ± 3.4	119.9 ± 1.6 ± 0.9	-3.9 ± 1.2 ± 0.6
1.0	1550.8 ± 4.0 ± 2.9	89.0 ± 1.2 ± 0.4	0.5 ± 0.8 ± 0.3
1.2	1631.6 ± 3.6 ± 2.2	61.9 ± 0.9 ± 0.6	1.9 ± 0.5 ± 0.2
1.5	1775.8 ± 3.0 ± 2.3	29.4 ± 0.6 ± 0.3	1.6 ± 0.2 ± 0.1

TABLE III: Breakdown of the systematic errors for the first moment, M_1, for $B \to X_c e\nu$ in the B meson rest frame for all 6 values of E_{cut}

E_{cut}[GeV]	M_1 [MeV] 0.4	M_1 [MeV] 0.6	M_1 [MeV] 0.8	M_1 [MeV] 1.0	M_1 [MeV] 1.2	M_1 [MeV] 1.5
electron identification	0.69	0.59	0.57	0.50	0.44	0.27
detection efficiency	0.00	0.00	0.00	0.00	0.00	0.00
$B \to D^{(*)} e\nu$ form factors	2.08	1.53	1.06	0.89	0.84	1.07
$B \to D^{(*)} e\nu$ Br	4.06	3.69	3.04	2.61	2.00	1.50
$B \to D^{(*)}_{(s)} \to e$ Br	0.21	0.18	0.13	0.08	0.05	0.01
continuum background	0.35	0.35	0.30	0.19	0.08	0.04
combinatorial background	0.01	0.06	0.06	0.04	0.03	0.06
hadron fakes	0.70	0.60	0.45	0.25	0.08	0.02
secondaries	1.99	0.79	0.67	0.49	0.01	1.30
unfolding	1.63	0.67	0.32	0.44	0.31	0.35
$b \to u$ subtraction	0.17	0.19	0.21	0.21	0.21	0.21
total systematics	5.38	4.27	3.37	2.94	2.20	2.30

A set of statistical correlation coefficients for all measured moments with E_{cut} ranging from 0.4 GeV to 1.5 GeV are given in Table VI.

SUMMARY

We report a measurement of the electron energy spectrum of the inclusive decay $B \to X_c e\nu$ and its first, second and third moments for threshold energies from 0.4 GeV to 1.5 GeV.

TABLE IV: Breakdown of the systematic errors for the second moment, M_2, for $B \to X_c e\nu$ in the B meson rest frame for all 6 values of $E_{\rm cut}$

$E_{\rm cut}$[GeV]	M_2 [10^{-3}GeV^2] 0.4	M_2 [10^{-3}GeV^2] 0.6	M_2 [10^{-3}GeV^2] 0.8	M_2 [10^{-3}GeV^2] 1.0	M_2 [10^{-3}GeV^2] 1.2	M_2 [10^{-3}GeV^2] 1.5
electron identification	0.31	0.26	0.2	0.15	0.11	0.05
detection efficiency	0.00	0.00	0.00	0.00	0.00	0.00
$B \to D^{(*)} e\nu$ form factors	0.81	0.43	0.32	0.29	0.27	0.16
$B \to D^{(*)} e\nu$ Br	0.18	0.07	0.22	0.22	0.22	0.10
$B \to D^{(*)}_{(s)} \to e$ Br	0.05	0.03	0.02	0.01	0.00	0.00
continuum background	0.12	0.10	0.06	0.03	0.02	0.00
combinatorial background	0.08	0.06	0.04	0.03	0.02	0.01
hadron fakes	0.17	0.12	0.07	0.03	0.01	0.00
secondaries	1.36	0.78	0.72	0.13	0.40	0.09
unfolding	1.43	0.78	0.25	0.16	0.20	0.21
$b \to u$ subtraction	0.13	0.11	0.09	0.08	0.07	0.06
total systematics	2.18	1.19	0.88	0.42	0.57	0.31

This set of moments, combined with the measurements of the semileptonic branching fraction and the moments of the hadronic mass distribution, will be used for the determination of the HQE parameters and of $|V_{cb}|$.

ACKNOWLEDGMENTS

We thank the KEKB group for the excellent operation of the accelerator, the KEK Cryogenics group for the efficient operation of the solenoid, and the KEK computer group and the National Institute of Informatics for valuable computing and Super-SINET network support. We acknowledge support from the Ministry of Education, Culture, Sports, Science, and Technology of Japan and the Japan Society for the Promotion of Science; the Australian Research Council and the Australian Department of Education, Science and Training; the National Science Foundation of China under contract No. 10175071; the Department of Science and Technology of India; the BK21 program of the Ministry of Education of Korea and the CHEP SRC program of the Korea Science and Engineering Foundation; the Polish State Committee for Scientific Research under contract No. 2P03B 01324; the Ministry of Science and Technology of the Russian Federation; the Ministry of Education, Science and Sport of the Republic of Slovenia; the National Science Council and the Ministry of Education of Taiwan; and the U.S. Department of Energy.

[1] I. Bigi, M. Shifman, and N. Uraltsev, Ann. Rev. Nuc. Part. Sci. **47** , 591 (1997)
[2] A. V. Manohar and M. B. Wise, Phys. Rev.**D49**, 110 (1994).

TABLE V: Breakdown of the systematic errors for the third moment, M_3, for $B \to X_c e\nu$ in the B meson rest frame for all 6 values of $E_{\rm cut}$

$E_{\rm cut}$[GeV]	M_3 [10^{-6}GeV^3] 0.4	M_3 [10^{-6}GeV^3] 0.6	M_3 [10^{-6}GeV^3] 0.8	M_3 [10^{-6}GeV^3] 1.0	M_3 [10^{-6}GeV^3] 1.2	M_3 [10^{-6}GeV^3] 1.5
electron identification	0.13	0.12	0.08	0.05	0.02	0.00
detection efficiency	0.00	0.00	0.00	0.00	0.00	0.00
$B \to D^{(*)} e\nu$ form factors	0.17	0.11	0.09	0.05	0.03	0.03
$B \to D^{(*)} e\nu$ Br	0.49	0.42	0.33	0.21	0.12	0.05
$B \to D^{(*)}_{(s)} \to e$ Br	0.02	0.02	0.01	0.01	0.00	0.00
continuum background	0.06	0.05	0.04	0.02	0.01	0.00
combinatorial background	0.02	0.02	0.01	0.00	0.00	0.00
hadron fakes	0.07	0.05	0.04	0.02	0.01	0.00
secondaries	0.35	0.44	0.41	0.20	0.05	0.00
unfolding	0.24	0.06	0.05	0.08	0.07	0.04
$b \to u$ subtraction	0.01	0.01	0.02	0.02	0.02	0.02
total systematics	0.72	0.63	0.55	0.31	0.15	0.07

[3] P. Gambino and N. Uraltsev, Eur. Phys. J. **C 34**, 181 (2004). See also C. Bauer, Z. Ligeti, M. Luke, A. Manohar, M. Trott Phys. Rev. **D 70**, 094017 (2004)

[4] M. Voloshin and M. Shifman, Sov. J. Nucl. Phys. , 292 (1987);
J. Chay, H. Georgi and B. Grinstein, Phys. Lett. B 247, 399 (1990);
I. Bigi, N. Uraltsev and A. Vainshtein, Phys. Lett. B 293, 430 (1992).

[5] M. Battaglia *et al.* (DELPHI Collaboration), DELPHI 2003-028 CONF 648.

[6] A. H. Mahmood *et al.* (CLEO Collaboration), submitted to Phys. Rev. D. [hep-ex/0403053]

[7] B. Aubert *et al.* (BABAR Collaboration), submitted to Phys. Rev. D. [hep-ex/0403030]

[8] K. Abe *et al.* (Belle Collaboration), BELLE-CONF-0474 [hep-ex/0409015]

[9] S. Kurokawa and E. Kikutani, Nucl. Instr. and. Meth. A499, 1 (2003), and other papers included in this volume.

[10] A. Abashian *et al.* (Belle Collaboration), Nucl. Instr. and Meth. A **479**, 117 (2002).

[11] Events are generated with the EVTGEN generator; the detector response is simulated with GEANT, R. Brun *et al.*, GEANT 3.21 CERN Report DD/EE/84-1, 1984.

[12] The selection of hadronic events is described in K. Abe *et al.* Belle Collaboration, Phys. Rev. **D 64**, 072001 (2001).

[13] Throughout this paper, the inclusion of the charge conjugate mode decay is implied unless otherwise stated.

[14] N. Isgur and D. Scora, Phys. Rev. **D 52**, 2783 (1995). See also N. Isgur *et al.*, Phys. Rev. **D 39**, 799 (1989).

[15] J. Duboscq *et al.* (CLEO Collaboration), Phys. Rev. Lett. **76**, 3898 (1996).

[16] J.L. Goity and W. Roberts, Phys. Rev. **D 51**, 3459 (1995).

[17] S. Eidelman *et al.*, Phys. Lett. B 592, 1 (2004).

[18] F. De Fazio and N. Neubert, JHEP **9906** (1999) 017.

TABLE VI: Correlation matrix for 18 measured moments. Correlation coefficients are statistical only.

	$M_1^{0.4}$	$M_1^{0.6}$	$M_1^{0.8}$	$M_1^{1.0}$	$M_1^{1.2}$	$M_1^{1.5}$	$M_2^{0.4}$	$M_2^{0.6}$	$M_2^{0.8}$	$M_2^{1.0}$	$M_2^{1.2}$	$M_2^{1.5}$	$M_3^{0.4}$	$M_3^{0.6}$	$M_3^{0.8}$	$M_3^{1.0}$	$M_3^{1.2}$	$M_3^{1.5}$
$M_1^{0.4}$	1.00	0.91	0.79	0.64	0.49	0.28	-0.28	-0.15	-0.05	0.01	0.03	0.03	0.85	0.62	0.42	0.25	0.14	0.04
$M_1^{0.6}$		1.00	0.87	0.71	0.54	0.31	-0.18	-0.19	-0.06	0.01	0.04	0.04	0.77	0.87	0.59	0.35	0.19	0.06
$M_1^{0.8}$			1.00	0.81	0.62	0.35	-0.06	-0.08	-0.08	0.01	0.05	0.06	0.70	0.77	0.88	0.53	0.28	0.08
$M_1^{1.0}$				1.00	0.77	0.43	0.01	0.01	0.02	0.01	0.07	0.08	0.56	0.62	0.71	0.89	0.46	0.14
$M_1^{1.2}$					1.00	0.56	0.05	0.06	0.07	0.08	0.12	0.12	0.43	0.46	0.53	0.66	0.86	0.25
$M_1^{1.5}$						1.00	0.08	0.09	0.10	0.13	0.16	0.29	0.23	0.25	0.30	0.36	0.47	0.83
$M_2^{0.4}$							1.00	0.80	0.60	0.41	0.27	0.11	-0.48	-0.22	-0.05	0.07	0.05	0.06
$M_2^{0.6}$								1.00	0.75	0.52	0.34	0.14	-0.25	-0.31	-0.06	0.04	0.06	0.08
$M_2^{0.8}$									1.00	0.69	0.44	0.19	-0.06	-0.08	-0.09	0.08	0.10	0.10
$M_2^{1.0}$										1.00	0.64	0.27	0.03	0.05	0.06	0.11	0.16	0.15
$M_2^{1.2}$											1.00	0.42	0.07	0.10	0.13	0.19	0.26	0.23
$M_2^{1.5}$												1.00	0.02	0.04	0.06	0.09	0.16	0.55
$M_3^{0.4}$													1.00	0.71	0.47	0.27	0.15	0.05
$M_3^{0.6}$														1.00	0.66	0.39	0.21	0.07
$M_3^{0.8}$															1.00	0.59	0.32	0.10
$M_3^{1.0}$																1.00	0.54	0.16
$M_3^{1.2}$																	1.00	0.30
$M_3^{1.5}$																		1.00

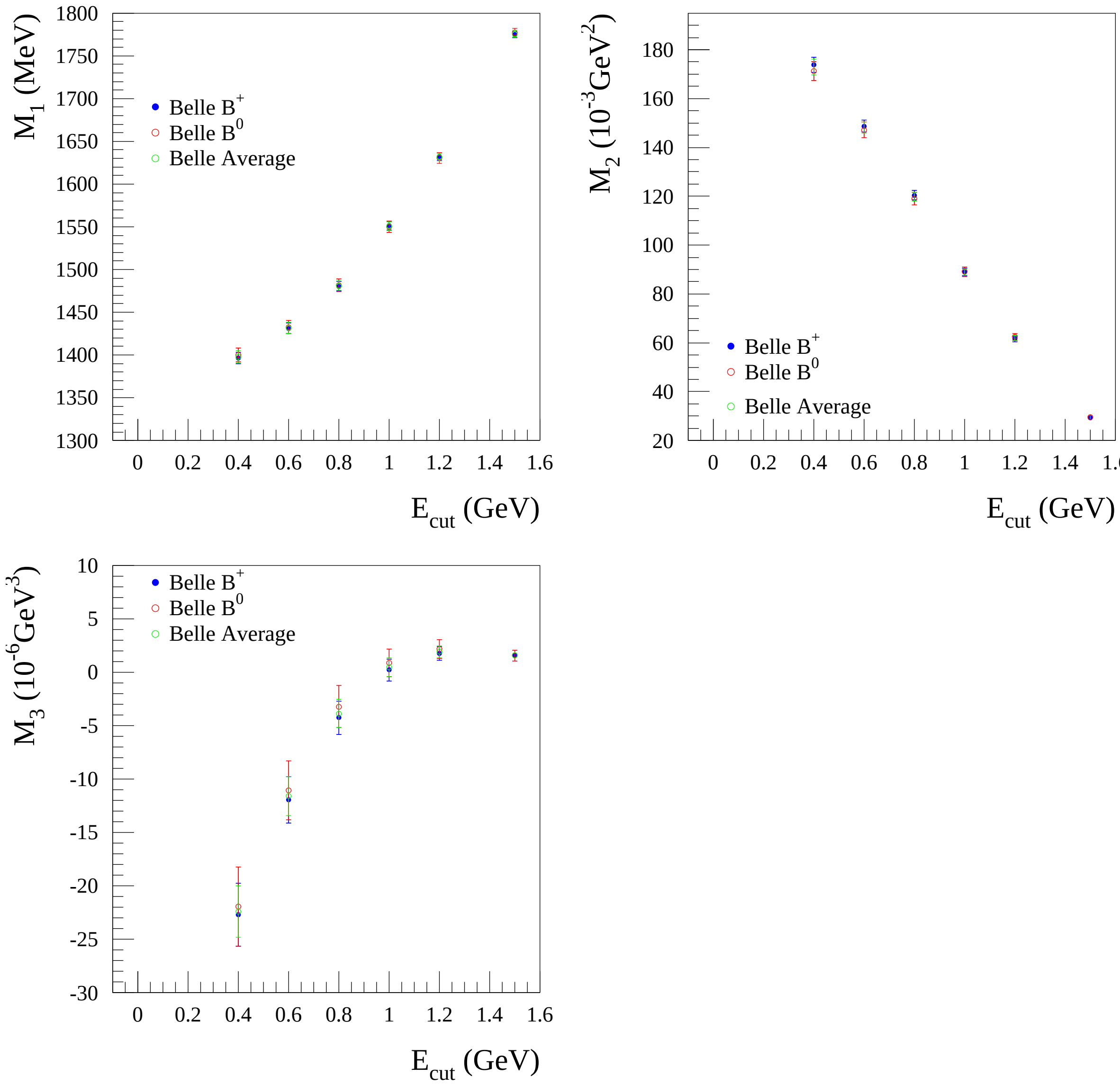

FIG. 3: First, second and third electron energy moments, M_1, M_2 and M_3, as a function of cutoff energy $E_{\rm cut}$. The errors shown are statistical and systematic.

[19] A. Limosani and T. Nozaki, [hep-ex/0407052]
[20] A. Höcker and V. Kartvelishvili, Nucl. Instr. Meth. **A372**, 469 (1996). [hep-ph/9509307]
[21] E. Barberio and Z. Was, Comp. Phys. Commun. **79**, 291 (1994).